

Effect of Asian Dust Storms on the Ambient SO₂ Concentration over North-East India: A Case Study

Timmy Francis

Physical Research Laboratory, Ahmedabad, India.
Email: timmyf@prl.res.in

Received May 3rd, 2011; revised June 12th, 2011; accepted July 21st, 2011.

ABSTRACT

Ambient SO₂ concentration at a high rain fall site, Shillong (25.67°N, 91.91°E, 1064 m ASL), located in North-East India, was measured during March 2009 and January 2010 with the aim to understand the effect of long range transport of pollutants from North-East Asia on the ambient SO₂ levels at this relatively clean site. The concentrations recorded during the former sampling period were very high (Max: 262.3 ppb)—which decayed down gradually towards the end the sampling period—whereas those during the latter sampling period were well within the acceptable limits (Max: 29.7 ppb). This elevated SO₂ concentrations during March 2009 is proposed to have association with a major cold air outbreak and an associated cyclone preceding one of the dust storm events reported in China, and a resultant sudden change in wind trajectory leading to the long range transport of pollutants to the sampling site. The argument is formulated on the basis of the back trajectory analysis performed using HYSPLIT for the month of March 2009—the plots clearly showed a drastic change in wind trajectories between 8th and 15th of March 2009 wherein the winds traveled over some of the highly polluted regions such as the Perm region of Russia—and on the results from model runs performed using the global 3-D model of tropospheric chemistry, GEOS-Chem (v8-03-01)—it clearly showed the tropospheric SO₂ over Perm region in Russia peaking during Nov, Dec, Jan, Feb and Mar every year, possibly due to central heating. The observation of long range transport of SO₂ from the highly industrialized areas of Perm in Russia to North-East India during dust storm events has important implications to the present understanding on its relative contribution to the Asian pollutant outflow to the Pacific during spring as the GEOS-Chem model runs also showed regions in and around Russia with relatively high concentrations of atmospheric NO_x, Peroxyacetyl Nitrate, Lumped Peroxypropionyl Nitrate, HNO₃, HNO₄, C₃H₈, C₂H₆, SO₄, NH₄, Inorganic Sulphur Nitrates and Lumped Alkyl Nitrate.

Keywords: SO₂, GEOS-Chem, HYSPLIT, Cold Air Outbreaks, Asian Dust Storms, Asian Pollutant Outflow

1. Introduction

Asian region is fast evolving as one of the major energy consuming regions in the world for a rapidly growing population and emerging economy [1], projected mega cities in Asia as one of the large emission sources of SO₂. As per IPCC 2007, there has been a regional shift in the emissions of SO₂ from US and Europe to South-East Asia, with implication to shift in atmospheric radiative forcing patterns for these regions [2-4]. In this scenario, monitoring ambient SO₂ concentration coupled with wind trajectory analysis in the North-East region of India—characterized by high rain fall—has special significance to assessing the role of long range transport from North-East Asia in controlling the pollutant characteristics over

this region. With this objective ambient SO₂ concentrations were measured during March 2009 and January 2010 at a high rainfall site in North-East India, Shillong (25.67°N, 91.91°E, 1064 m Above Sea Level (ASL)).

2. Materials and Methods

2.1. Site Description: Shillong (25.67°N, 91.91°E, 1064 m ASL)

The sampling site (25.67°N, 91.91°E, 1064 m ASL) is located about 18 km away from the Shillong city, located on the Shillong Plateau which is an outlier of the plateau of peninsular India and is composed primarily of ancient rocks. The highest point is Shillong peak, at 1961 m ASL located 5 km south of the city of Shillong. It is on

the Shillong Plateau, the only major pop-up structure in the northern Indian shield. Due to its latitude and high elevation Shillong has a sub-tropical climate with mild summers and chilly to cold winters. The region is subject to vagaries of the monsoon. The average annual rain fall is about 2200 mm. The monsoon arrives in June and it rains almost until the end of August. Perched at an altitude of 1521 m ASL, the Shillong city stretches for about 6 km on an elevated tract. The city is situated on a plateau bound on the north by the Umiam gorge, on the northwest by the great mass of the Diengiei Hills that rise up to a height of 1852 m ASL, and on the northeast by the hills of the Assam valley. The proximity of this high rainfall site to some of the highly polluted regions in North-East Asia and hence the possibility of long range transport makes this study location strategically important.

2.2. Experiment: SO₂ Monitoring System

The experimental set up comprised of a primary UV fluorescence SO₂ Monitor (Thermo—43i Trace Level Enhanced (TLE)), an air compressor for producing zero-level (zero) gas and a dynamic gas calibrator (Thermo—146i) for preparing diluted SO₂ standard gas. Using pulsed fluorescence technology, the Model 43i-TLE measures the amount of sulfur dioxide in the air with an instrumental detection limit of 50 pptv (300 second averaging time). The UV fluorescence SO₂ monitor was calibrated onsite every 10 days with standard SO₂ gas (2 ppmv with N₂ balance gas, Spectra, USA) and zero air. Five minute averaged SO₂ raw data was accumulated in the SO₂ analyzer which in turn was periodically downloaded and fed to a computer through an ethernet port. Discussions on the performances of similar systems can be seen elsewhere [5-7].

2.3. The HYSPLIT Trajectory Model

The HYSPLIT (HYbrid Single-Particle Lagrangian Integrated Trajectory) model, developed by NOAA ARL [8,9], was used for the back trajectory analysis for this work. HYSPLIT uses a modeled vertical velocity scheme; it can depict the vertical motion of the relevant air parcel. The model computes the advection of a single pollutant particle, or simply its trajectory.

2.4. GEOS-Chem Model Description

2.4.1. General Description

The GEOS-Chem global 3-D model of tropospheric chemistry (v8-03-01; <http://acmg.seas.harvard.edu/geos/>) driven by GEOS-5 assimilated meteorological observations from the NASA Global Modeling and Assimilation Office (GMAO) is employed for this work. Meteorological fields in the GEOS-5 have 6-h temporal resolution (3-hour resolution for surface fields and mixing

depths) and a horizontal resolution of 0.5° latitude × 0.667° longitude, with 72 levels in the vertical extending from the surface to approximately 0.01 hPa. The model is applied to a global simulation of Ozone-NO_x-VOC-aerosol chemistry. General descriptions of GEOS-Chem are given by [10] and [11]. The detailed descriptions of the GEOS-Chem aerosol emission inventories and simulation evaluations are provided in [11] and [12] for sulfur and ammonia, in [13] for dust, and in [14] for recent updates on emission inventories over the China region. The simulations were conducted for January-December 2009 at 4° × 5° resolutions. They were initialized on 1st January 2009 using GEOS-Chem fields generated by a one year spin-up simulation with 4° × 5° resolution.

2.4.2. Emission Inventories Included in the Model Runs

In the Model runs, the following emission inventories were used:

- 1) The EMEP—the Co-operative Programme for Monitoring and Evaluation of the Long-range Transmission of Air Pollutants in Europe—inventory for 2000 [15].

- 2) The Big Bend Regional Aerosol and Visibility Observational (BRAVO) study inventory for 1999 [16].

- 3) The global sulfur emission based on the Emissions Database for Global Atmospheric Research (EDGAR) inventory [17].

- 4) The Streets inventory [18].

- 5) The Canada Criteria Air Contaminants (CAC) inventory for 2002

(http://www.ec.gc.ca/pdb/cac/cac_home_e.cfm) and

- 6) The Environmental Protection Agency (EPA/NEI05) inventory.

The bio-fuel emissions and biogenic emissions also were included in the model runs with the Model of Emissions of Gases and Aerosols from Nature (MEGAN) v2.1 [19] inventory used for the latter.

2.5. GAMAP Visualization Toolkit

The Global Atmospheric Model Analysis Package (GAMAP) (Version 2.15; <http://acmg.seas.harvard.edu/gamap/>) is used for plotting the output from the GEOS-Chem runs. GAMAP is a self-contained, consistent, and user-friendly software package for reading and visualizing output from Chemical Tracer Models (CTM's) and consists of a suite of routines written in IDL (Interactive Data Language). It can produce line plots, 2D plots, 2D animations, or 3D iso-contour surface plots and can read 2D, 3D or 4D data blocks.

3. Results and Discussions

Ambient SO₂ concentrations were measured during

March 2009 and January 2010 at the high rainfall site, Shillong (25.67°N, 91.91°E, 1064 m ASL) in North-East India, using the pulsed UV fluorescence analyzer. During the measurements the inlet of the SO₂ analyzer was maintained at an altitude of about 15 m above the ground, while the analyzer was housed in an air conditioned room. The integration time for the analyzer was set at 5 minutes. An Automated Weather Station (AWS) located within a distance of 1/2 km from the sampling site was employed to monitor the various atmospheric parameters such as the wind speed, wind direction, relative humidity, atmospheric pressure etc, throughout the sampling period.

3.1. Major Features during March 2009

Figure 1 reveals the temporal changes of the SO₂ concentrations at Shillong, during March 2009. The concentration levels recorded during the initial days of the sampling were very high (Max: 262.3 ppb) which decayed down gradually towards the end the sampling period.

This observed high SO₂ concentrations is explained as due to a transient long range pollutant transport from North-East Asia associated with the cold air outbreak preceding the dust storm events reported in China [20] on 14th March 2009 and in North-East India [21] on 17th March 2009. The former [20], using MODIS 1B data of relevant regions, showed evidences for the dust storm in western Gansu and Neimenggu in China while the latter [21], based on Terra/Aqua MODIS data, reported the dust storm over Guwahati, North-East India. Based on the mesoscale model (MM5) derived wind speed directions at 850 hPa overlaid on sea level pressure on 17th March 2009, [21] found a persistent North-Easterly flow with high wind speed (~6 m/s) over the region resulting in mobilization and lifting of dust particles in to the atmosphere. They analyzed NCEP temperature/relative humidity (RH) anomalies variations and found ~0.6°C increase in surface air temperature and ~-4% reduction in RH during March 2009, which they said has resulted in dry conditions over the region. They attributed the very high value of Terra MODIS AOD₅₅₀ (~1.3) along with lower value of Alpha (~0.78) to coarse mode dust aerosol particles over the region due to dust event occurred on 17th March 2009.

The above argument of long range transport as the mechanism responsible for the observed high SO₂ values at the North-East Indian sampling site is based on the results provided collectively by the back trajectory analysis performed using HYSPLIT for the sampling period and the model runs performed using the Chemical Transport Model GEOS-Chem. The arguments are further supported with the local meteorological parameters measured using nearby Automated Weather Station

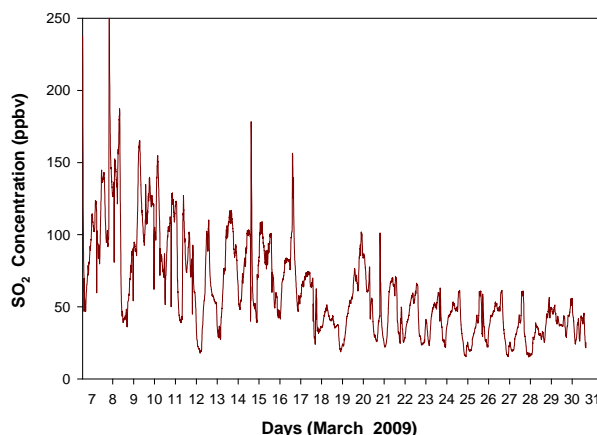


Figure 1. The measured SO₂ time series profile during March 2009 at the sampling site, Shillong.

(AWS). The time series Mineral Dust Optical Depth (MOPD) profiles created using GEOS-Chem (discussed in the following sections) for the month of March 2009 also gave evidence for the dust storm movement reported in China on 14th March 2009.

3.1.1. Interpreting the High SO₂ Values

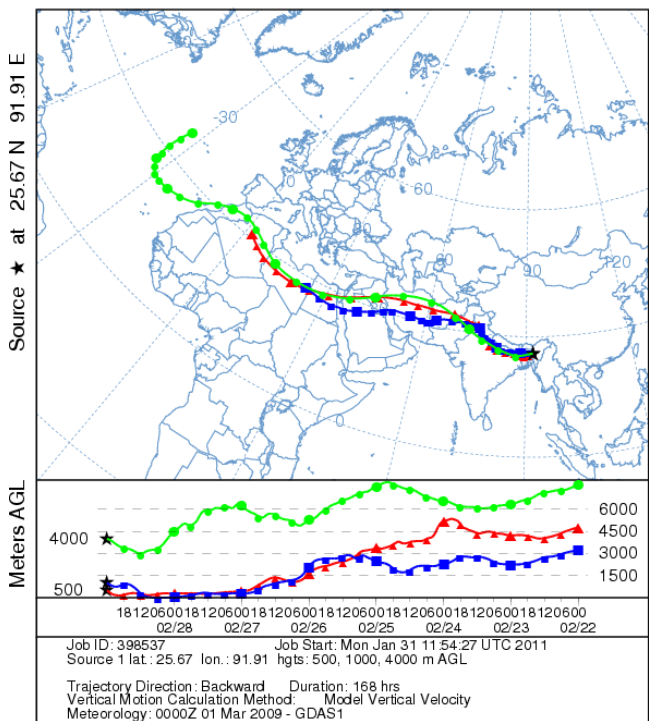
3.1.1.1. Source Identification Based on HYSPLIT Trajectories

The 7 days back trajectories beginning from the sampling site were generated (**Figure 2**) using HYSPLIT for whole the sampling month, with one trajectory plot made each on 1st, 8th, 15th, 22nd and 29th of March 2009. The trajectories computed to identify the source regions were for altitudes 500 m, 1000 m and 4000 m Above Ground Level (AGL). The plots showed clearly that between 8th and 15th of March 2009 there was a drastic change in wind trajectories. During this period the winds which were traveling in the eastward direction suddenly got bend and started traveling towards North-East till it reach ~60°N and from there it again got bend and started traveling towards the south to reach the sampling site. It was in line with this observed sudden change in the wind trajectory (between 8th and 15th of March 2009), the high SO₂ concentrations were recorded. The back trajectories plotted for the following weeks again showed wind patterns similar to the ones persisted prior 8th March 2009. The observed decay in concentration levels during the days succeeding the transient long range pollutant transport were in line with this normal trajectory pattern.

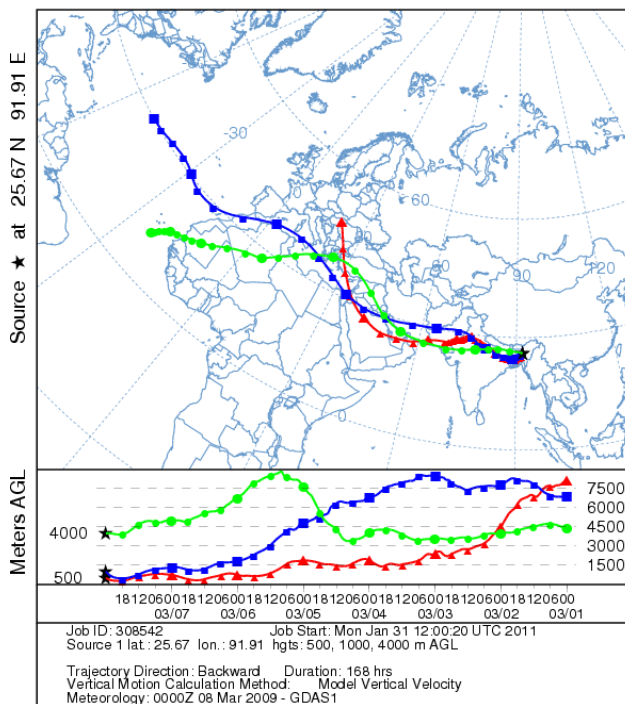
3.1.1.2. Source Identification Using GEOS-Chem Model

The GEOS-Chem model (v8-03-01) was run from 1st January 2009 to 31st December 2009, after spinning up the model fields for one year, and the output averaged for the first half of each month was generated. The results were then plotted using GAMAP to find out the possible

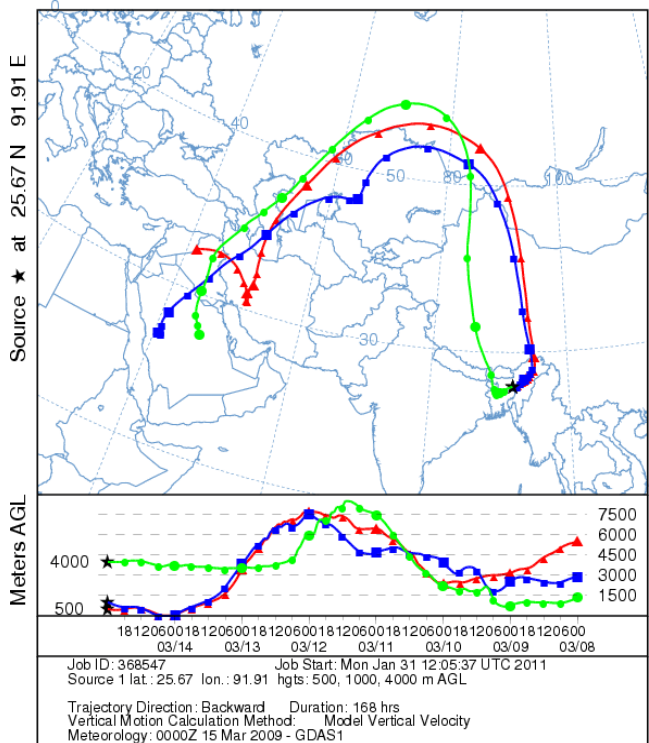
NOAA HYSPLIT MODEL
Backward trajectories ending at 0000 UTC 01 Mar 09
GDAS Meteorological Data



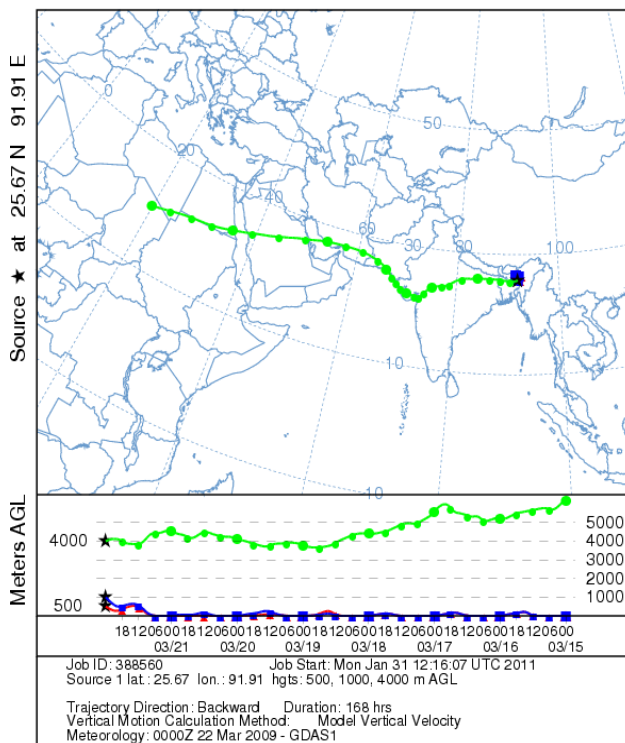
NOAA HYSPLIT MODEL
Backward trajectories ending at 0000 UTC 08 Mar 09
GDAS Meteorological Data



NOAA HYSPLIT MODEL
Backward trajectories ending at 0000 UTC 15 Mar 09
GDAS Meteorological Data



NOAA HYSPLIT MODEL
Backward trajectories ending at 0000 UTC 22 Mar 09
GDAS Meteorological Data



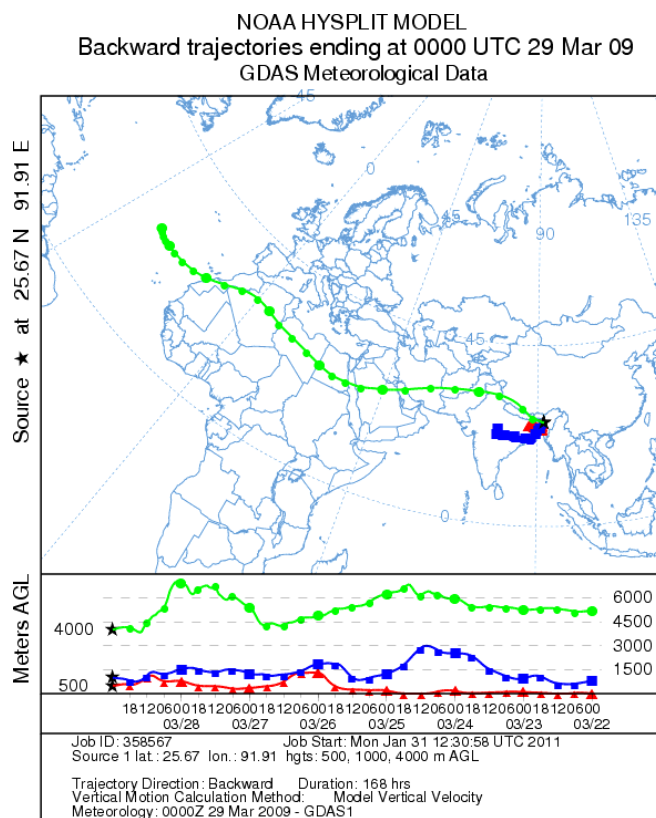


Figure 2. The 7-day back trajectories originating at the sampling site plotted using HYSPLIT for March 2009.

SO₂ source regions along the back trajectories obtained between 8th and 15th of March 2009. The plots clearly showed that many of the regions over which the winds traveled during this period are characterized by high concentrations of SO₂. Out of these the Perm region in Russia has the highest SO₂ concentration in the GEOS-Chem generated plots.

3.1.1.2.1. The Perm City, Russia

Perm, projected in this paper as the source region for the high SO₂ containing air parcel detected at the sampling site, is a city in the eastern part of Russia, near the Urals Mountains. It is a major center of heavy industries, chemical industries (varnishes, paints, fertilizers, sulfuric acid, etc.), petrochemical and oil refining industries, defense production, timber and wood processing industries, food industry and so on. This regional area has substantial deposits of natural resources (oil, gas, potassium, magnesium salt, precious and jobbing stones, gold and chromium ores and so on.) which is the base for both the extractive industries and related economic sectors of the region. The region of Perm has one of the richest mineral resource bases in Russia and has many mines.

The Perm region is known for its long frosty, snowy Ural winters. However, the region's severe continental climate causes abrupt seasonal changes, from a cold

winter followed by a mild, usually warm spring and then by a hot summer. The cold winter necessitates central heating especially during the months November, December, January, February, and March. The general precipitation trend over Perm region shows lowest precipitation events during the months February and March followed by slightly higher precipitation events in April.

3.1.1.3. Anomalies Detected in Local Meteorology

The Automated Weather Station (AWS)—located within 500m from the sampling location—provided meteorological parameters such as wind speed & wind direction (**Figure 3**), relative humidity (**Figure 4**) and atmospheric pressure (**Figure 5**) throughout the month of March 2009 except for a small non-operational period from 20 - 23rd March 2009. Statistically the wind direction mostly remained South-East with second directional preference for South-West. The wind speed showed a transient increase between 9th and 13th of March 2009 with the maximum speed recorded of 3.2 m/s. The relative humidity (RH) remained more or less on the higher side throughout the sampling period with a small dip recorded between 10th and 12th followed by two spikes each on 13th and 14th. The highest RH value observed for the month was on 17th with the peak relative humidity value recorded of 99%. The Atmospheric pressure also kept

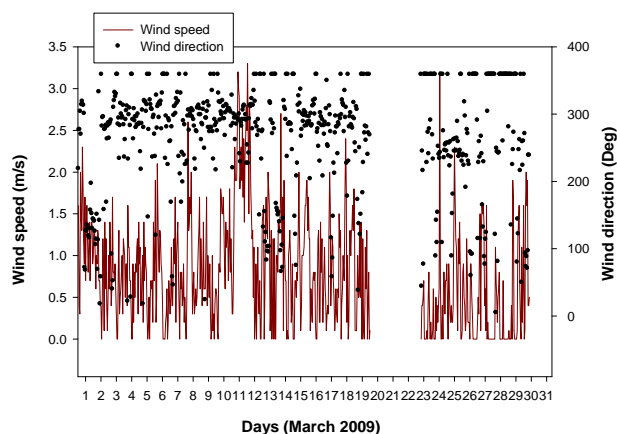


Figure 3. Wind speed and wind direction during the sampling period, obtained from nearby AWS.

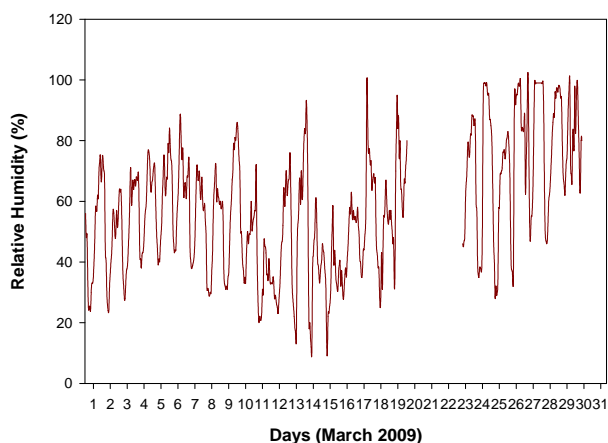


Figure 4. Relative humidity during the sampling period, obtained from nearby AWS.

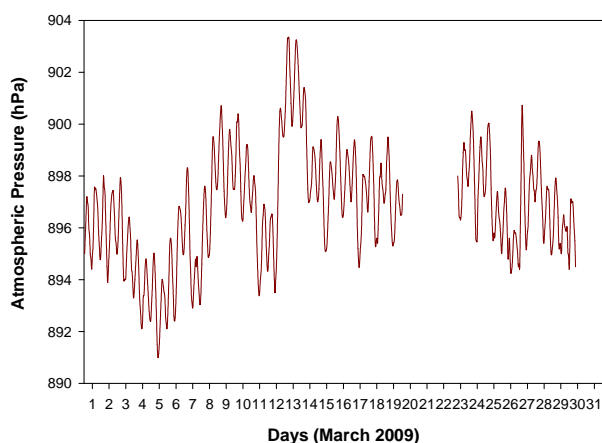


Figure 5. Atmospheric pressure during the sampling period, obtained from nearby AWS.

unusually fluctuating with a dip observed between 3rd and 7th (lowest value 891 hPa) and a hump observed

between 12th and 15th of March 2009 (Max value 903.3 hPa).

3.1.1.4. Dust Storm Detection Using GEOS-Chem

To visualize and understand the source and the trajectory of the dust storms reported [20] in China on 14th March 2009 and over North-East India [21] on 17th March 2009, the GEOS-Chem model was run with the inventories discussed previously, and generated the time series Mineral Dust Optical Depth (MOPD) data for the month of March 2009. The plots generated from these data for the days 10th to 20th of March 2009 (**Figure 6**) clearly showed this formation and the movement of the dust storm. The plots also showed high MOPD values for the Indo-Gangetic Plane also during 13th and 14th March 2009. A second phase of high MOPD values for North-East India started on 17th March 2009 which remained high in the following few days (18th, 19th and 20th March 2009).

3.1.1.4.1. Cold Air Outbreaks and Dust Storms in Asia

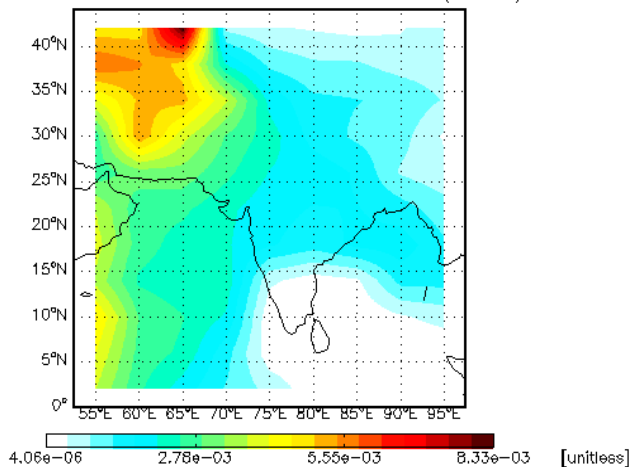
It is known that Asian dust storms, especially those of Chinese origin occur during spring [22], when the climate over East Asia reaches its maximum dryness of the year, the surface start warming, and strong winds sweep over the desert areas leading to highly unstable synoptic systems. The percentages of dust storms generally occurring in China during March, April, and May are 20%, 58%, and 22%, respectively [23].

Asian dust storms are always associated with cold air outbreaks, resulting in the Mongolian cyclonic depression and frontal system. It is known that polar front causes mid-latitude jet stream (by the thermal wind relationship) with troughs and ridges to lead to patterns of divergence aloft. This upper air disturbance causes a significant pressure decrease in the lower atmosphere as a result of cyclogenesis, leading to the development of a low pressure system with low central sea level pressures which continue to deepen as time progress to cause cyclone and a resulting dust mobilization.

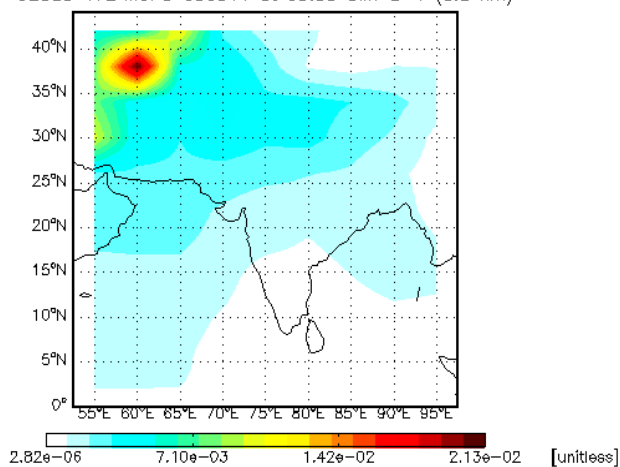
The reason the sampling was planned during this season at this North-Eastern Indian site was to understand the possible effects of such cold air outbreaks and the associated atmospheric disturbance preceding the Chinese dust storms in altering the atmospheric pollutant transport pattern to North-East India.

To visualize this air disturbance associated with the cold air outbreak occurred during the above sampling period, trajectory matrices were plotted on 8th, 11th, 15th, 22nd and 29th of March 2009 with source at multiple locations (**Figure 7**). The plots clearly indicated a major atmospheric disturbance between 8th and 15th of March 2009.

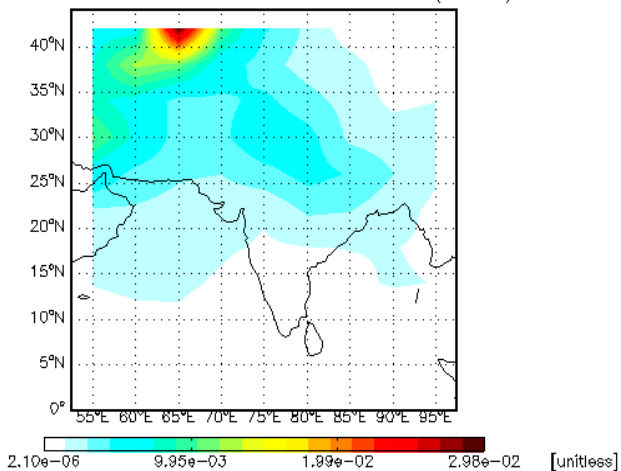
GEOS5 47L MOPD 090310 at 09:59 GMT L=1 (0.3 km)



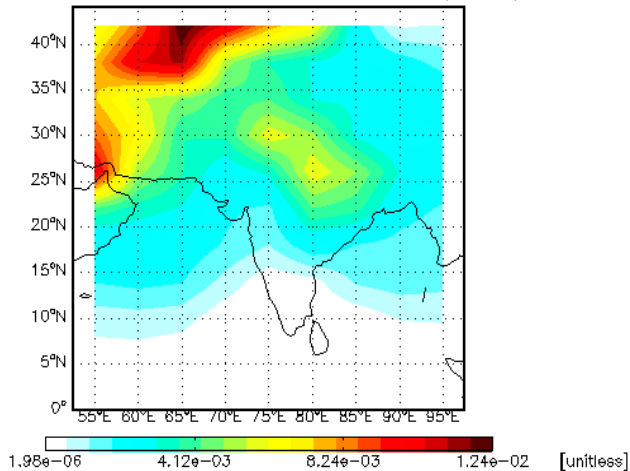
GEOS5 47L MOPD 090311 at 09:59 GMT L=1 (0.3 km)



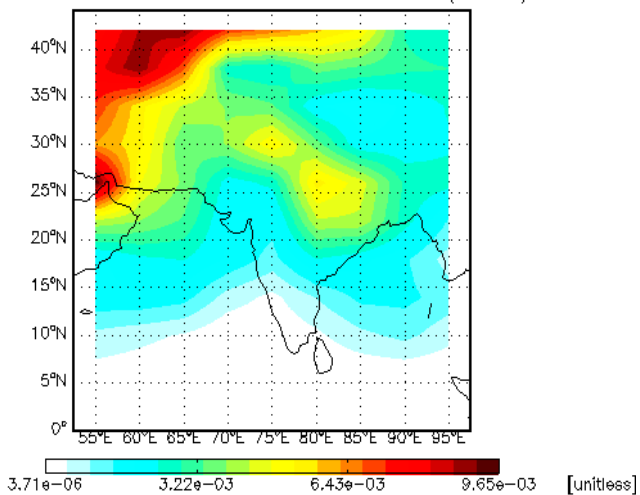
GEOS5 47L MOPD 090312 at 09:59 GMT L=1 (0.3 km)



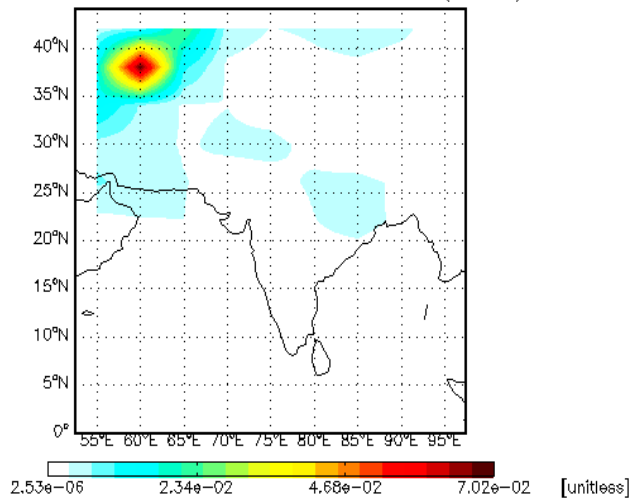
GEOS5 47L MOPD 090313 at 09:59 GMT L=1 (0.3 km)



GEOS5 47L MOPD 090314 at 09:59 GMT L=1 (0.3 km)



GEOS5 47L MOPD 090315 at 09:59 GMT L=1 (0.3 km)



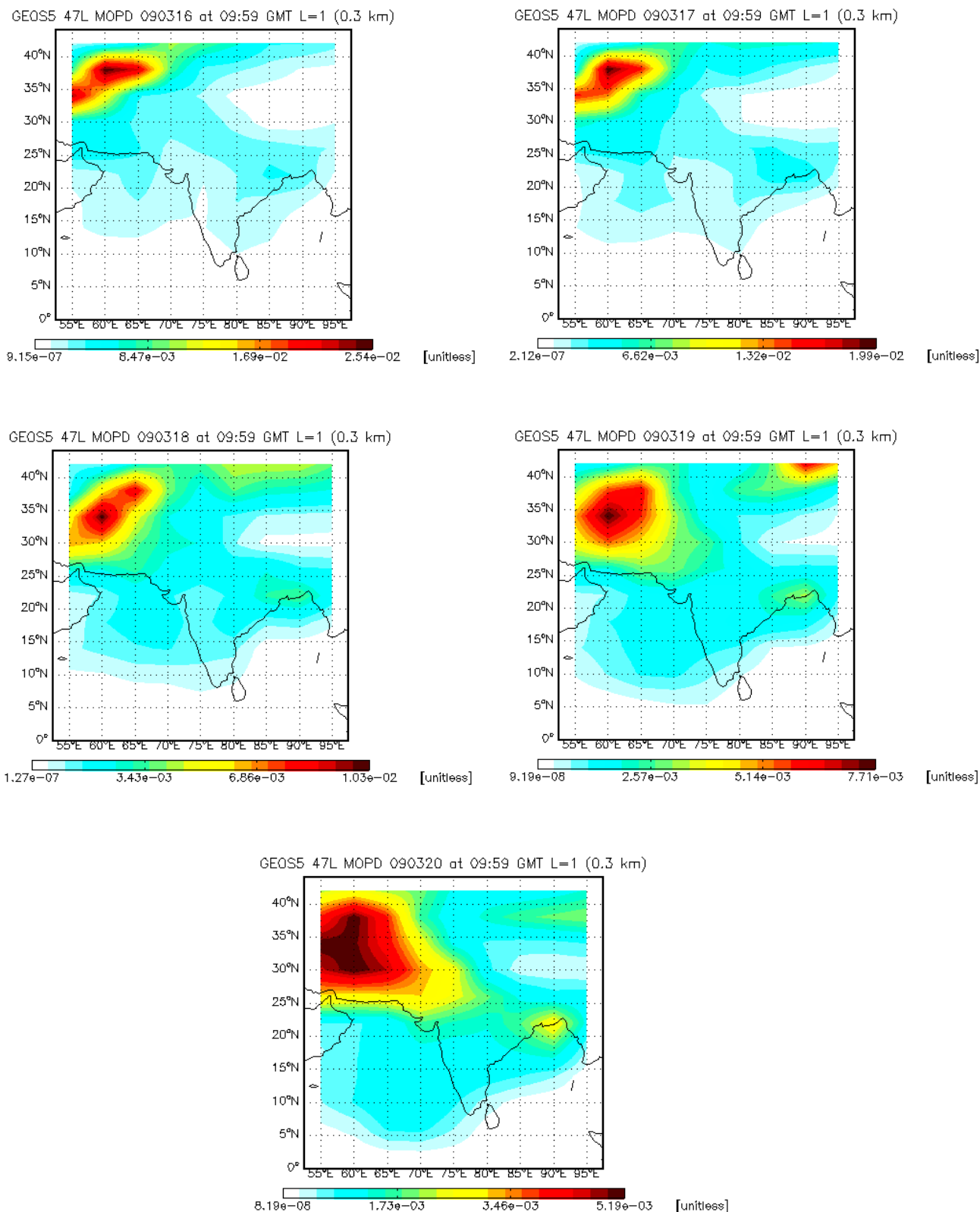
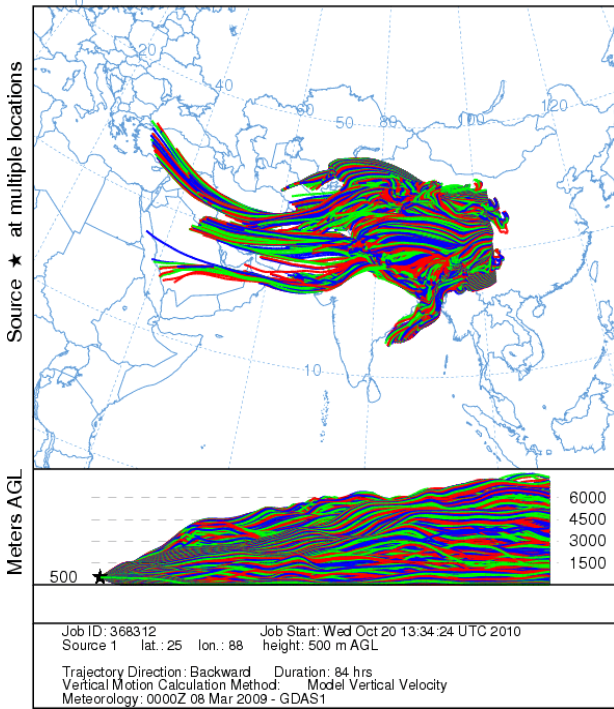
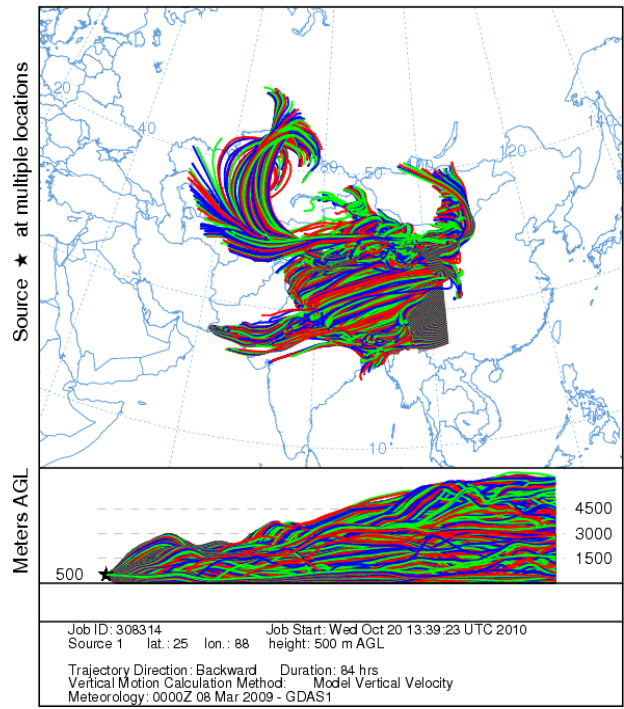


Figure 6. The Mineral Dust Optical Depth (MOPD) profile obtained during 10th to 20th of March 2009 from GEOS-Chem.

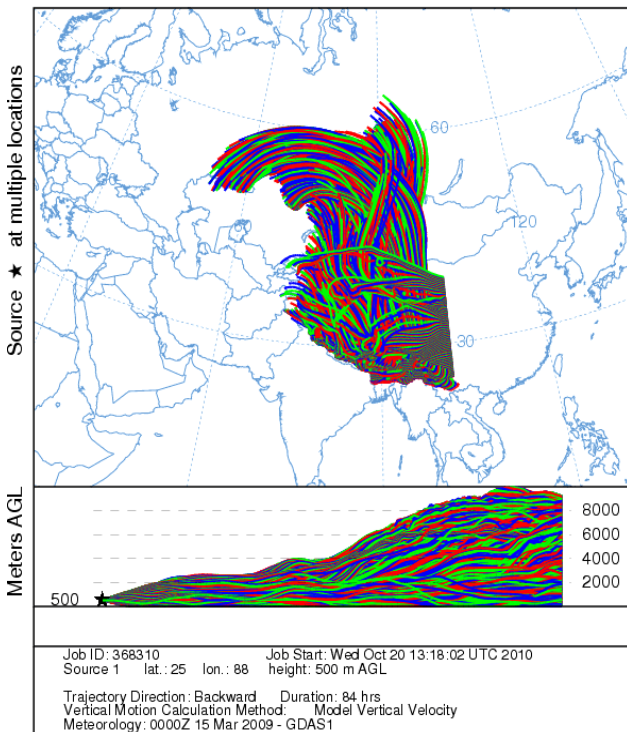
NOAA HYSPLIT MODEL
Backward trajectories ending at 0000 UTC 08 Mar 09
GDAS Meteorological Data



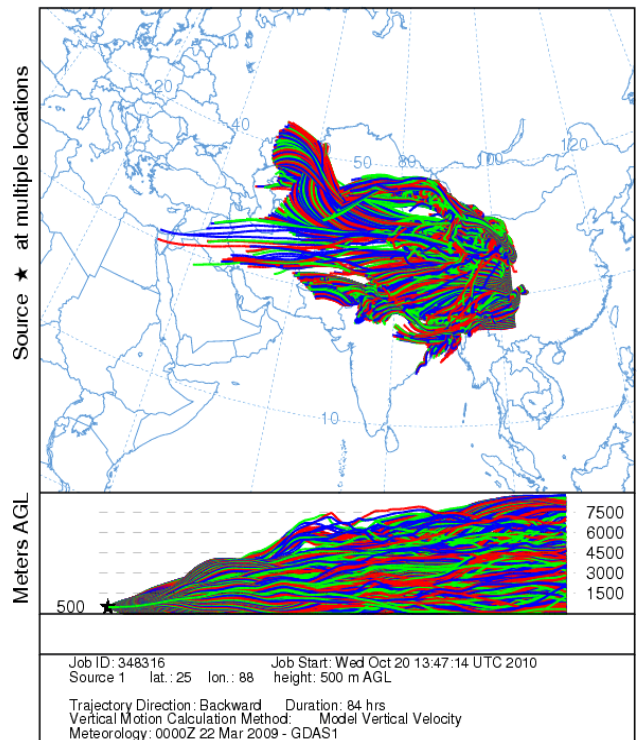
NOAA HYSPLIT MODEL
Backward trajectories ending at 0000 UTC 11 Mar 09
GDAS Meteorological Data



NOAA HYSPLIT MODEL
Backward trajectories ending at 0000 UTC 15 Mar 09
GDAS Meteorological Data



NOAA HYSPLIT MODEL
Backward trajectories ending at 0000 UTC 22 Mar 09
GDAS Meteorological Data



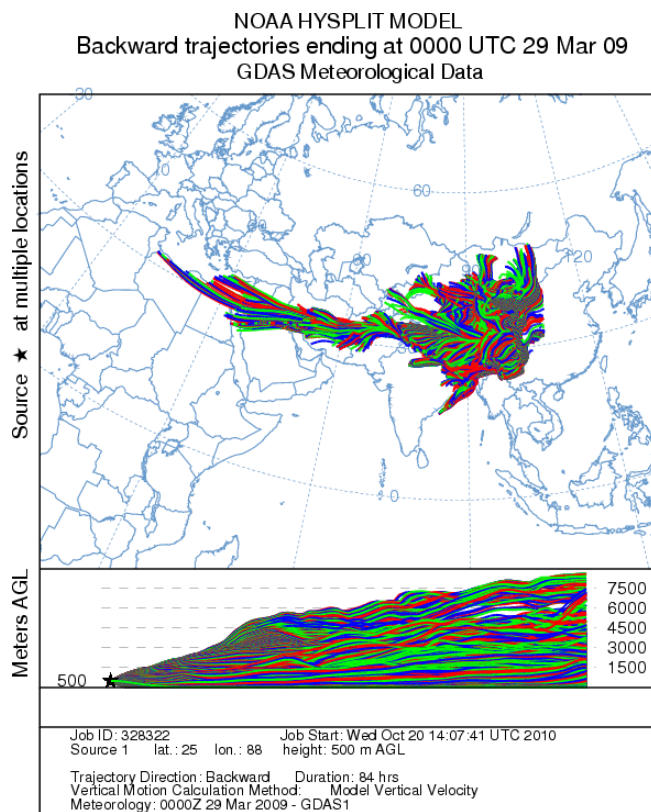


Figure 7. The Trajectory Matrix plotted using HYSPLIT for the cold air out break period.

3.2. Transport from Russian Region: Implication to the Asian Pollutant Outflow

The observation that SO₂ got transported from the highly industrialized areas of Perm in Russia to North-East India during the dust storm event in March 2009 has important implications to its share in the Asian pollutant outflow to the Pacific during spring, every year. To make this picture clear, 7 day back trajectories starting at coordinates (18°N, 130°E) and (22°N, 110°E), (**Figure 8**) were plotted which showed the air parcel from Russian region reaching the Pacific during the dust storm days. Based on these observations, it is projected here that the contribution from this region is non negligible while assessing the impact of Asian pollutant outflow, as the Perm region is characterized by a wide range of industries.

The GEOS-Chem generated SO₂ plots for every month (averaged over the first 15 days) plotted for the whole year 2009 (**Figure 9**) clearly showed the tropospheric SO₂ over Perm region peaking during November, December, January, February and March every year, possibly because of central heating. The lesser amount of precipitation in the Perm region during the months February and March result in longer atmospheric retention time for these pollutants during these months. The concentration

levels go decreasing when there is increase in precipitation events starting from April along with the receding winter to reduce the central heating requirements.

The model runs were also performed to find out the concentration levels of other major pollutants over this region during March 2009. It was found that regions in and around Russia has relatively high concentrations of atmospheric NO_x, Peroxyacetyl Nitrate (PAN), Lumped Peroxypropionyl Nitrate (PPN), HNO₃, HNO₄, C₃H₈, C₂H₆, SO₄, NH₄, Inorganic Sulphur Nitrates (NIT), and Lumped Alkyl Nitrate (R₄N₂) (**Figure 10**).

The model runs also showed (figures not included here) that similar to SO₂, these pollutants also peak during November, December, January, February, and March every year, again possibly has association with central heating and climatology discussed above. But the fact that cold air outbreaks preceding the dust storm events in Asia occur only during March, April and May makes the relative contribution from this region significant only during March, when the atmospheric pollutant peak for the region overlaps with the dust storm months (March, April, May). So it suggest that during the dust storm events in March, the contribution from regions in and around Russia may not be neglected while considering the impact of Asian pollutant outflow to the Pacific, which becomes less significant during cold air outbreaks and the associated dust

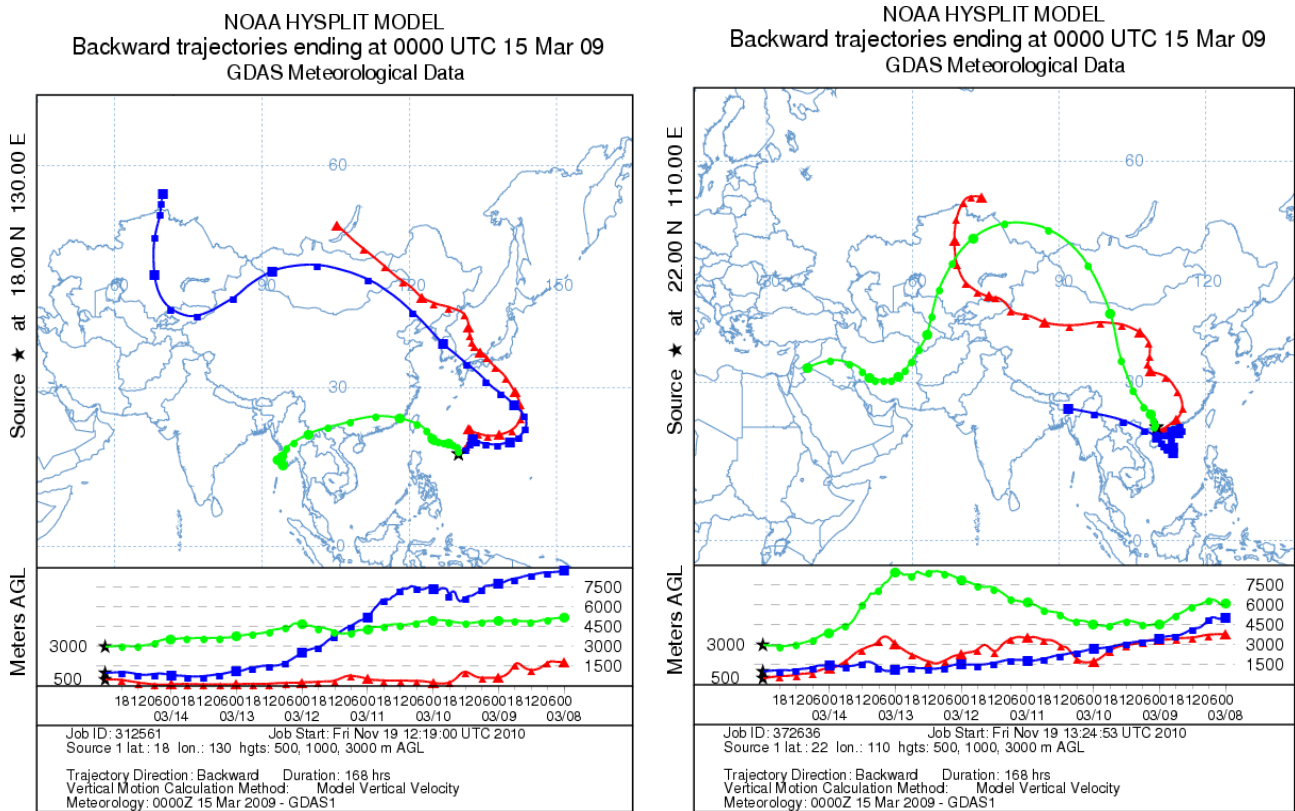
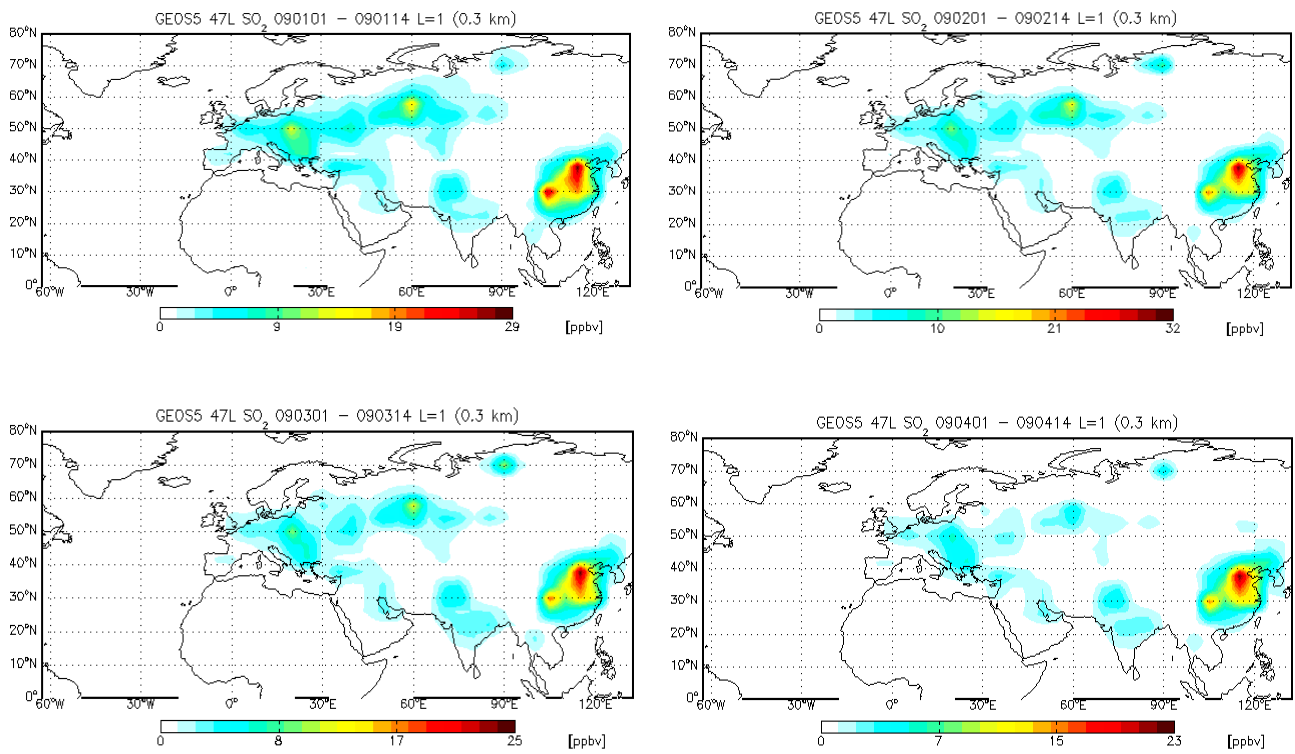


Figure 8. The 7-day back trajectories showing the air parcel from Russian region reaching the Pacific during the dust storm events.



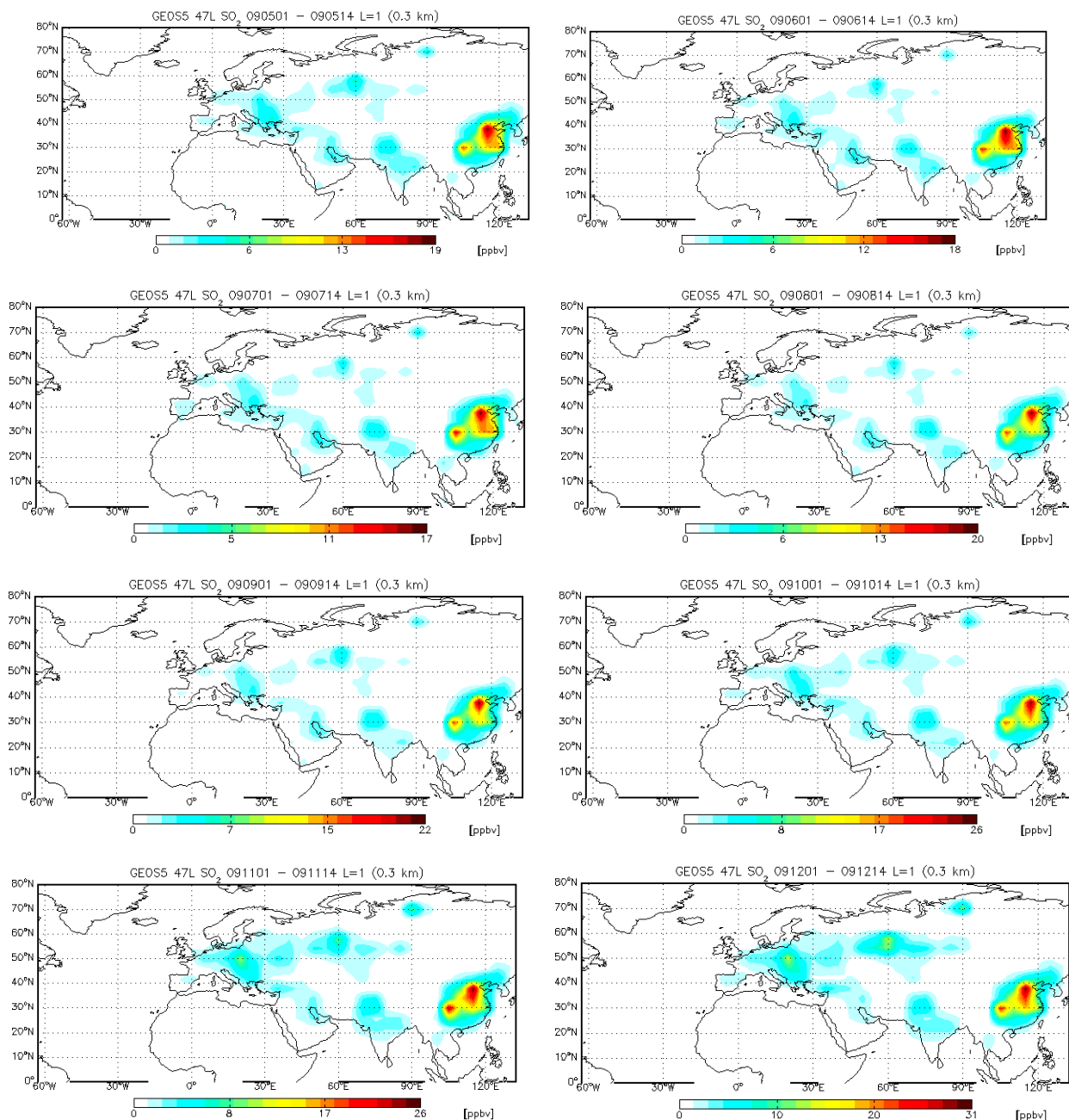
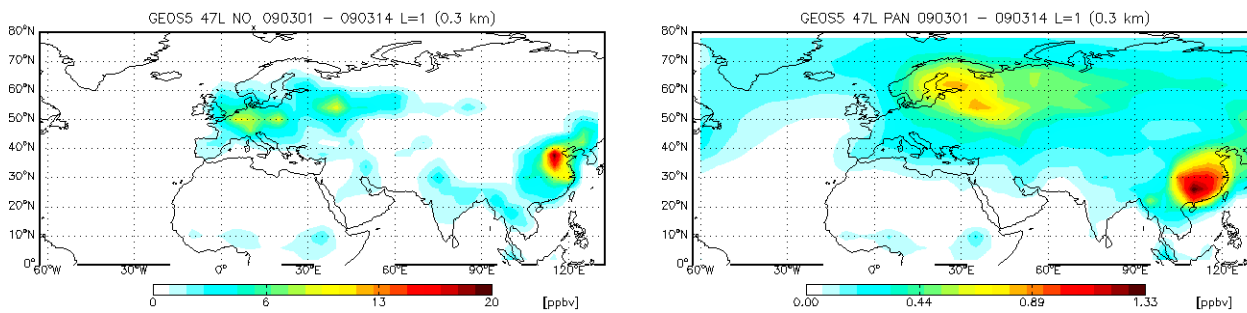


Figure 9. SO₂ profile averaged for the first half of every month for 2009 from GEOS-Chem model runs showing the SO₂ peaking over the Perm region in Russia, during the months November, December, January, February and March.



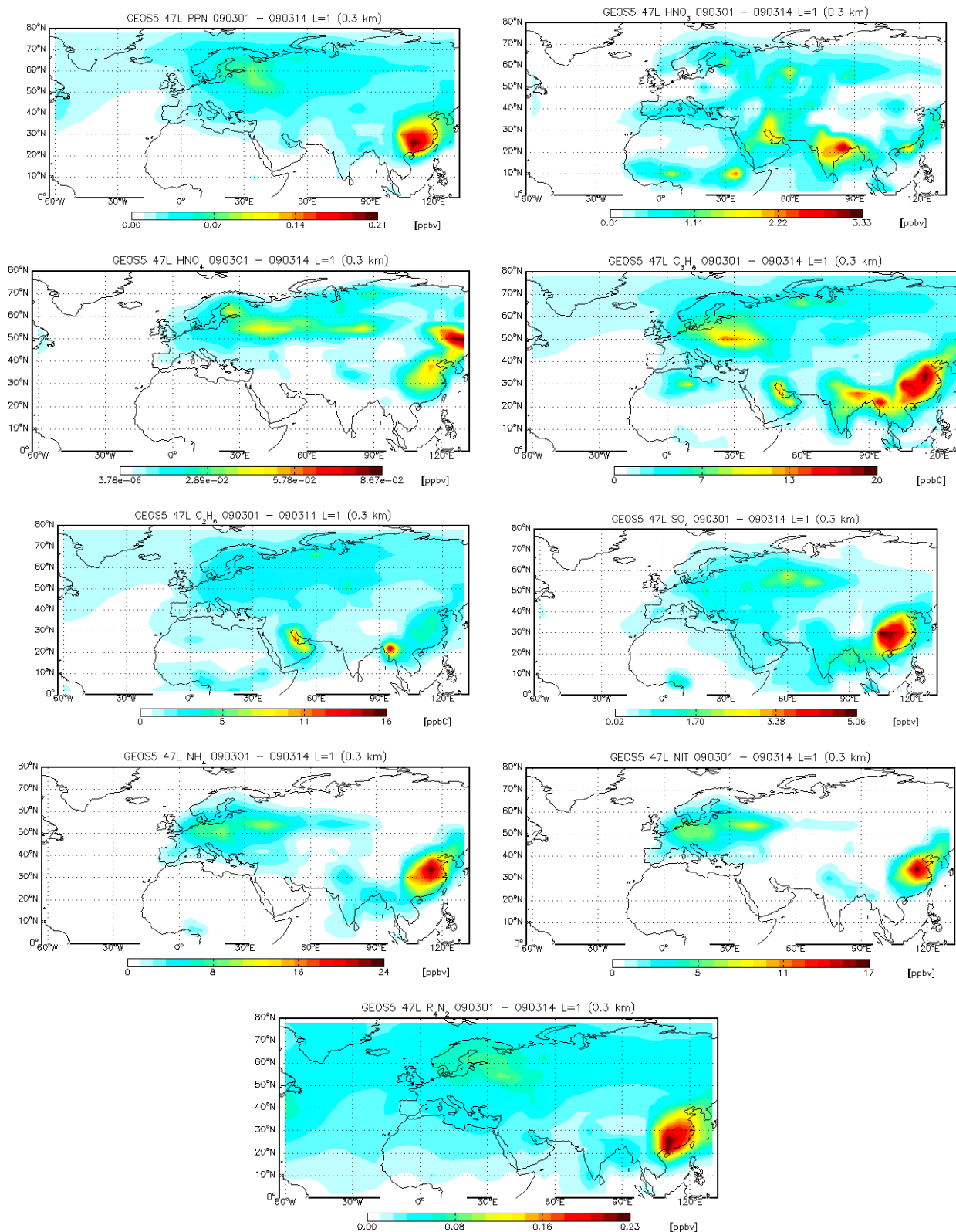


Figure 10. NO_x, Peroxyacetyl Nitrate (PAN), Lumped Peroxypropionyl Nitrate (PPN), HNO₃, HNO₄, C₃H₈, C₂H₆, SO₄, NH₄, Inorganic Sulphur Nitrates (NIT) and Lumped Alkyl Nitrate (R₄N₂) profiles averaged for the first half of March 2009 from GEOS-Chem model runs.

storms happening in April, and May.

The model runs also showed (**Figure 11**) that the pollutants N₂O₅, NH₃, hydrophilic black carbon, hydrophilic organic carbon, hydrophobic black carbon and hydrophobic organic carbon are present only in smaller levels in the Perm region compared to the other known polluted regions in North East Asia, and so are not expected to contribute significantly to the Asian pollutant outflow.

3.3. SO₂ Time-Series Data (March 2009): Model Versus Observations

Figure 12 shows the time series SO₂ profile obtained for the nearest co-ordinates (26°N, 90°E) from the GEOS-Chem model runs for the month of March 2009. The model was not able to pick up the magnitude of this major transport event even though a slight increase in the

SO₂ levels were observed between 8th and 16th of March 2009 and in general the concentrations resembled more or less to the background levels expected for this high rainfall site in the absence of long range transports.

3.4. Major Features during January 2010

Unlike March 2009 the SO₂ concentrations recorded during January 2010 (**Figure 13**) were well within the acceptable limits, with maximum value going up to 29.7 ppb only and a minimum value recorded of 1.94 ppb. The wind back trajectory analysis (**Figure 14**) showed that the winds were coming from West Asian region and had no component coming from North-East Asia ruling out the possibility of any long range transport from Russia. So the concentration levels recorded may be taken as the background SO₂ values for this North-Eastern Indian site.

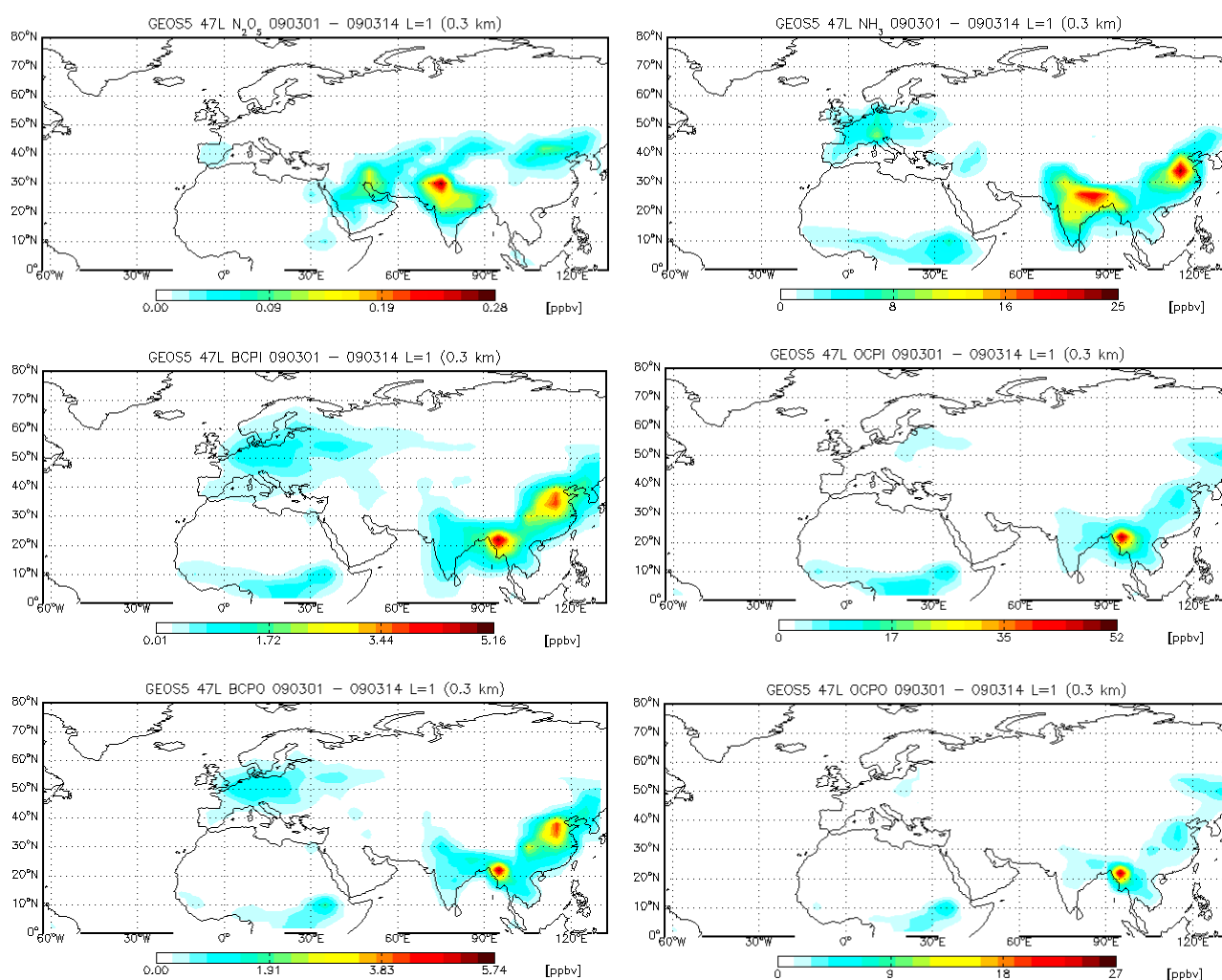


Figure 11. N₂O₅, NH₃, hydrophilic black carbon (BCPI), hydrophilic organic carbon (OCPI), hydrophobic black carbon (BCPO), hydrophobic organic carbon (OCPO) profiles averaged for the first half of March 2009 from GEOS-Chem model runs.

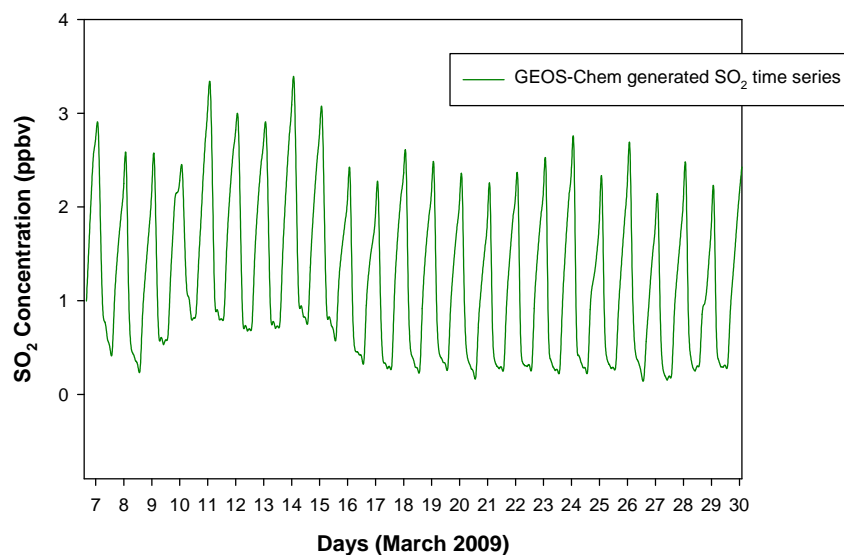


Figure 12. SO₂ time series profile generated using GEOS-Chem for the sampling period in March 2009 for the nearest co-ordinates (26°N, 90°E).

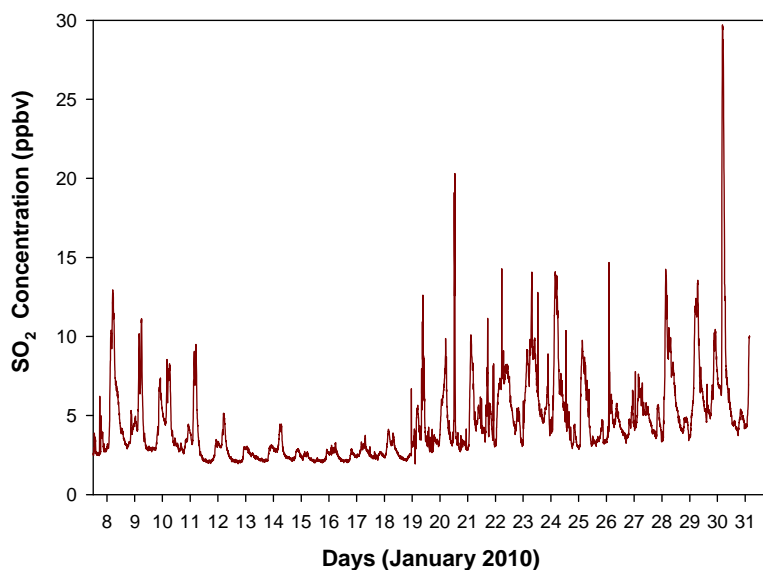


Figure 13. The measured SO₂ time series profile during January 2010 at the sampling site, Shillong.

3.5. SO₂ Time-Series Data (January 2010): Model Versus Observations

In the case of January 2010, the time series output from the model (Figure 15) matched more or less with the observations both magnitude wise and to certain extent shape wise. The diurnal variation observed in the experimental data is reproduced in the model generated time series output.

4. Conclusions

Ambient SO₂ concentrations at Shillong (25.67°N,

91.91°E, 1064 m ASL), a high rain fall site located in North East India, measured during March 2009 and January 2010 showed significant differences in magnitude, with concentrations going to a maximum of 262.3 ppb during the former sampling period—which decayed down gradually towards the end the sampling period - against the maximum value recorded during the latter period of 29.7 ppb. This elevated SO₂ concentrations during March 2009 is explained as due to a long range transport associated with the cold air outbreak preceding one of the dust storm events reported in China. This argument of long range transport for the observed high SO₂

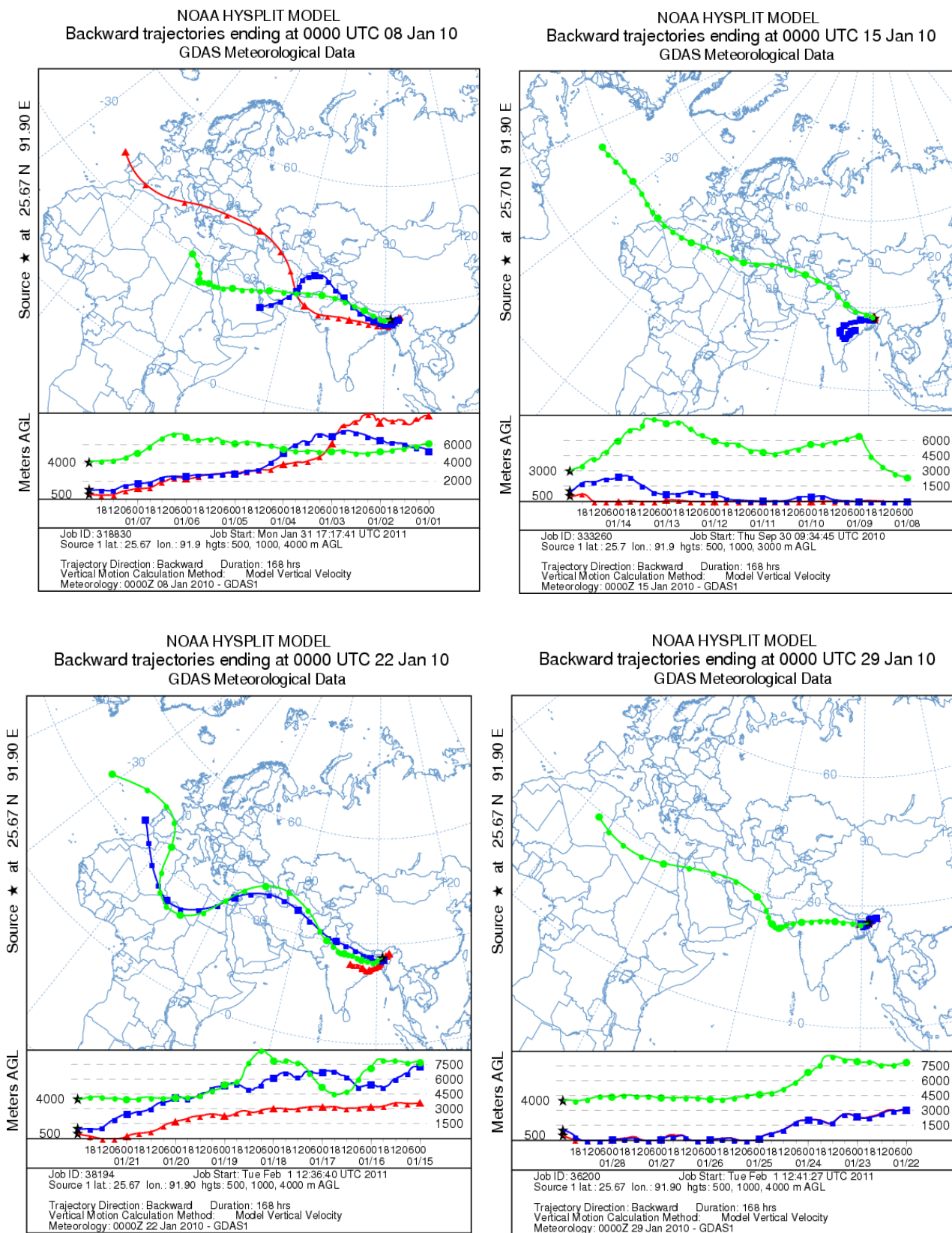


Figure 14. The 7-day back trajectories originating at the sampling site plotted using HYSPLIT for January 2010.

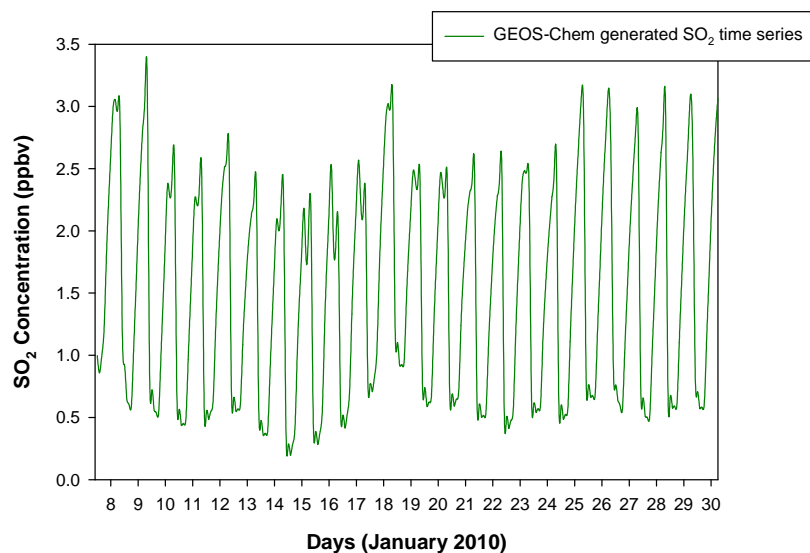


Figure 15. SO₂ time series profile generated using GEOS-Chem for the sampling period in January 2010 for the nearest co-ordinates (26°N, 90°E).

values during March 2009 is formulated on the basis of the back trajectory analysis performed using HYSPLIT for the sampling period—the plots clearly showed a drastic change in wind trajectories between 8th and 15th of March 2009 wherein the winds travelled over some of the highly polluted regions such as the Perm region of Russia—and on the basis of the results from simulations performed using the global 3-D model of tropospheric chemistry, GEOS-Chem (v8-03-01)—it clearly showed the tropospheric SO₂ over Perm region peaking during November, December, January, February and March every year, possibly due to central heating.

The observation of long range transport of SO₂ from the highly industrialized areas of Perm in Russia to North-East India during the dust storm event in March 2009 is projected to have important implications to its share in the Asian pollutant outflow to the Pacific during spring, every year. Separate runs of the model revealed that the regions in and around Russia have high concentrations of other atmospheric pollutants such as NO_x, Peroxyacetyl Nitrate, HNO₃, Lumped Peroxypropionyl Nitrate, HNO₃, HNO₄, C₃H₈, C₂H₆, SO₄, NH₄, Inorganic Sulphur Nitrates and Lumped Alkyl Nitrate. The model runs also showed that some of the other atmospheric pollutants such as N₂O₅, NH₃, hydrophilic black carbon, hydrophilic organic carbon, hydrophobic black carbon and hydrophobic organic carbon are present only in negligible levels in the Perm region compared to the other polluted regions in North-East Asia and so will not contribute significantly to the Asian pollutant outflow.

The comparison of the time series SO₂ profile obtained for the nearest co-ordinates (26°N, 90°E) from the

GEOS-Chem model with the experimental data, for the month of March 2009, revealed that the model was not able to pick up the magnitude of this transport whereas there is a good correlation between the two for January 2010.

5. Acknowledgements

The ISRO-Geosphere Biosphere Program (Department of Space, Government of India) is gratefully acknowledged for the partial financial support for this study. The author thanks Prof. M. M. Sarin, Physical Research Laboratory, India, for valuable scientific discussions and support during the course of this study. The author also like to thank Dr. P. P. Nageshwara Rao, Mr. S. S. Kundu, and Mr. Arup Borgohain (North Eastern Space Applications centre, ISRO), for the logistics provided, during the sampling at NESAC, Shillong.

REFERENCES

- [1] S. K. Guttikunda, G. R. Carmichael, G. Calori, *et al.*, “The Contribution of Megacities to Regional Sulfur Pollution in Asia,” *Atmospheric Environment*, Vol. 37, No. 1, 2003, pp. 11-22. [doi:10.1016/S1352-2310\(02\)00821-X](https://doi.org/10.1016/S1352-2310(02)00821-X)
- [2] O. Boucher and M. Pham, “History of Sulfate Aerosol Radiative Forcings,” *Geophysical Research Letters*, Vol. 29, No. 9, 2002, p. 1308. [doi:10.1029/2001GL014048](https://doi.org/10.1029/2001GL014048)
- [3] M. Pham, O. Boucher and D. Hauglustaine, “Changes in Atmospheric Sulfur Burdens and Concentrations and Resulting Radiative Forcings under IPCC SRES Emission Scenarios for 1990–2100,” *Journal of Geophysical Research*, Vol. 110, No. D6, 2005, p. D06112. [doi:10.1029/2004JD005125](https://doi.org/10.1029/2004JD005125)
- [4] S. J. Smith, E. Conception, R. Andres, *et al.*, “Historical

- Sulphur Dioxide Emissions 1850-2000: Methods and Results,” *Research Report*, No. PNNL-14537, Pacific Northwest National Laboratory, Richland, 2004.
- [5] Y. Igarashi, Y. Sawa, K. Yoshioka, *et al.*, “Monitoring the SO₂ Concentration at the Summit of Mt. Fuji and a Comparison with Other Trace Gases during Winter,” *Journal of Geophysical Research*, Vol. 109, No. D17, 2004, pp. 1-21. [doi:10.1029/2003JD004428](https://doi.org/10.1029/2003JD004428)
- [6] W. T. Luke, “Evaluation of a Commercial Pulsed Fluorescence Detector for the Measurement of Low-Level SO₂ Concentrations during the Gas-Phase Sulfur Inter-comparison Experiment,” *Journal of Geophysical Research*, Vol. 102, No. D13, 1997, pp. 16255-16265. [doi:10.1029/96JD03347](https://doi.org/10.1029/96JD03347)
- [7] M. Luria, J. F. Boatman, J. Harris, *et al.*, “Atmospheric Sulfur Dioxide at Mauna Loa, Hawaii,” *Journal of Geophysical Research*, Vol. 97, No. D5, 1992, pp. 6011-6022.
- [8] R. R. Draxler and G. D. Rolph, “HYSPLIT (Hybrid Single-Particle Lagrangian Integrated Trajectory) Model,” NOAA, Air Resources Laboratory, Silver Spring, 2011. <http://www.arl.noaa.gov/ready/hysplit4.html>
- [9] G. D. Rolph, “Real-Time Environmental Applications and Display System (READY),” NOAA Air Resource Lab, Silver Spring, Md, 2003. <http://www.arl.noaa.gov/ready/hysplit4.html>
- [10] I. Bey, D. J. Jacob, R. M. Yantosca, *et al.*, “Global Modeling of Tropospheric Chemistry with Assimilated Meteorology: Model Description and Evaluation,” *Journal of Geophysical Research*, Vol. 106, No. D19, 2001, pp. 23073-23095. [doi:10.1029/2001JD000807](https://doi.org/10.1029/2001JD000807)
- [11] R. J. Park, D. J. Jacob, B. D. Field, *et al.*, “Natural and Transboundary Pollution Influences on Sulfate-Nitrate-Ammonium Aerosols in the United States: Implications for Policy,” *Journal of Geophysical Research*, Vol. 109, No. D15, 2004, CiteID: D15204.
- [12] J. Wang, D. J. Jacob and S. T. Martin, “Sensitivity of Sulfate Direct Climate Forcing to the Hysteresis of Particle Phase Transitions,” *Journal of Geophysical Research*, Vol. 113, No. D11, 2008, pp. D11207.1-D11207.15.
- [13] T. D. Fairlie, D. J. Jacob and R. J. Park, “The Impact of Transpacific Transport of Mineral Dust in the United States,” *Atmospheric Environment*, Vol. 41, No. 6, 2007, pp. 1251-1266. [doi:10.1016/j.atmosenv.2006.09.048](https://doi.org/10.1016/j.atmosenv.2006.09.048)
- [14] D. Chen, Y. Wang, M. B. McElroy, *et al.*, “Regional CO Pollution and Export in China Simulated by the High-Resolution Nested-Grid GEOS-Chem Model,” *Atmospheric Chemistry and Physics*, Vol. 9, No. 11, 2009, pp. 3825-3839.
- [15] V. Vestreng and H. Klein, “Emission Data Reported to UNECE/EMEP. Quality Assurance and Trend Analysis and Presentation of WebDab,” *MSC-W Status Report 2002*, Norwegian Meteorological Institute, Oslo, 2002.
- [16] H. Kuhns, M. Green and V. Etyemezian, “Big Bend Regional Aerosol and Visibility Observational (BRAVO) study emissions inventory,” Desert Research Institute, Las Vegas, 2003.
- [17] J. G. J. Olivier and J. J. M. Berdowski, “Global Emissions Sources and Sinks, in the Climate System,” Balkema Publishers/Swets & Zeitlinger Publishers, Lisse, 2001, pp. 33-78.
- [18] D. G. Streets, Q. Zhang, L. Wang, *et al.*, “Revisiting China’s CO Emissions after the Transport and Chemical Evolution over the Pacific (TRACE-P) Mission: Synthesis of Inventories, Atmospheric Modeling, and Observations,” *Journal of Geophysical Research*, Vol. 111, No. D14, 2006, Cite ID: D14306.
- [19] A. Guenther, T. Karl, P. Harley, *et al.*, “Estimates of Global Terrestrial Isoprene Emissions Using MEGAN (Model of Emissions of Gases and Aerosols from Nature),” *Atmospheric Chemistry and Physics*, Vol. 6, No. 11, 2006, pp. 3181-3210. [doi:10.5194/acp-6-3181-2006](https://doi.org/10.5194/acp-6-3181-2006)
- [20] X. Li, and W. Song, “Dust Storm Detection Based on Modis Data,” *International Archives of Photogrammetry, Remote Sensing and Spatial Information Sciences*, Liaoning Technology University, Shengyang, pp. 169-172.
- [21] A. R. Sharma, S. K. Kharol and K. V. S. Badarinath, “An Unusual Dust Event over North-Eastern India and Its Association with Extreme Climatic Conditions—A Study Using Satellite Data,” *Aerosols & Clouds: Climate Change Perspectives*, ISATA Bulletin, 2000, pp. 214-217.
- [22] T. S. Liu, “Loess and the Environment,” China Ocean, Beijing, 1985, pp. 251.
- [23] J. Sun, M. Zhang and T. Liu, “Spatial and Temporal Characteristics of Dust Storms in China and its Surrounding Regions, 1960-1999: Relations to Source Area and Climate,” *Journal of Geophysical Research*, Vol. 106, No. D10, 2001, pp. 10325-10333. [doi:10.1029/2000JD900665](https://doi.org/10.1029/2000JD900665)